Moheb Fam[1] *and Carlos Santamarina*[1]

Study of Geoprocesses with Complementary Mechanical and Electromagnetic Wave Measurements in an Oedometer

REFERENCE: Fam, M. and Santamarina, C., "**Study of Geoprocesses with Complementary Mechanical and Electromagnetic Wave Measurements in an Oedometer,**" *Geotechnical Testing Journal,* GTJODJ, Vol. 18, No. 3, September 1995, pp. 307–314.

ABSTRACT: Particulate geomaterials can be uniquely studied with wave-based techniques. Electromagnetic and mechanical waves interact with the tested material, exciting different phenomena and revealing different information. Complementary wave measurements were implemented in a modified oedometric cell to study and to monitor different processes in geomaterials. The cell and the measuring devices are discussed, followed by a presentation of typical measurements conducted during consolidation, chemical diffusion, and cementation. The paper also includes a discussion of the most common computations and analyses involved in this type of test.

KEYWORDS: mechanical waves, electromagnetic waves, oedometer, clays, consolidation, diffusion, cementation

Soils are particulate media, therefore their properties are governed by interparticle forces. In the case of coarse-grained soils (e.g., gravels and sands), forces can be analyzed as large-scale mechanical-Newtonian interactions. At very small scales, e.g., fine clays, interparticle forces must be analyzed at the level of electrostatic-Coulombian interactions. The higher the specific surface of particles, the more significant the effect of surface processes on volumetric behavior and the higher the need for charge-based interpretation of observed geophenomena.

The propagation of low-energy electromagnetic and mechanical waves is a small, temporary perturbation to the material. At the macro level, mechanical waves produce shear distortion and volumetric changes, while electromagnetic waves result in polarization. Differences at the micro level are more subtle: mechanical waves change interatomic distances, preserving local electroneutrality (piezoelectricity requires special consideration); on the other hand, electromagnetic waves result in relative displacement of negative and positive charges, leading to local and global polarization of the material. Frequency-dependent polarization and deformation processes and geometry-dependent scattering and diffraction effects result in dispersive wave propagation. Therefore, wave spectra manifest inherent properties of the material.

Low-energy waves traverse materials without causing appreciable permanent changes. Given the particulate nature of soils and the corresponding difficulties with sampling and instrumentation, wave techniques present unique advantages to study geoprocesses without affecting the measured properties. Hence, waves can be used to characterize geomaterials and to study on-going physico-chemical processes.

The purpose of this paper is to introduce the methodology, to describe the device, and to present selected results for several studies on consolidation, concentration diffusion, and cementation. Complete data sequences and analyses can be found in Fam (1995), Santamarina and Fam (1995), and Fam and Santamarina (1995). Fundamental concepts in soil-wave interaction are reviewed first.

Soil-Wave Interaction

Electromagnetic Waves: Dielectric Permittivity

Electromagnetic waves are preferred to study materials that possess distinguishable electrical properties (e.g., an electrolyte plume in water-saturated sand) or materials that are affected by electromagnetic fields such as clays. The propagation of electromagnetic waves disturbs electrical charges and dipoles inside the material and at interfaces; the polarizability and the losses that characterize each polarization mechanism provide microlevel information about the material.

When a dielectric material is inserted between the electrodes of a capacitor (with initial charge in vacuum of Q_0) and the capacitor is still connected to the power supply, the charge on its surface increases to $Q_0 + \Delta Q$. This increase in charge reflects the compensation of some free charges on the surface of the electrodes by bound charges within the dielectric. Bound charges become aligned with the field, and the dielectric is "polarized." Polarization in a steady state field arises from a finite relative displacement of charges and is defined as the number of dipole moments per unit volume

$$P = \frac{\sum_{i=1}^{n} q \cdot x}{\delta v} \tag{1}$$

where q is the charge, x is the charge separation, δv is the volume, and n is the number of molecules per unit volume. The dipole moment is a function of the local electric field E. Let's assume a linear relationship between P and E

$$P = \alpha \cdot n \cdot E \tag{2}$$

where the linearity coefficient α is the "polarizability" of the polarizing unit. Finally, the relative permittivity κ' represents the

[1]Graduate student and associate professor, respectively, Civil Engineering Department, University of Waterloo, Waterloo, Canada N2L 3G1.

global polarizability of the material, and it is related to microparameters n and α by the Clausius-Mossotti equation

$$\kappa' = \frac{1 + \left(\frac{2}{3\epsilon_0} \cdot n \cdot \alpha\right)}{1 - \left(\frac{n \cdot \alpha}{3\epsilon_0}\right)} \tag{3}$$

If a capacitor is filled with a lossy material, the Ohmic current component appears in phase with the voltage. When the direction of the field changes rapidly, electrical charges are unable to follow the change in the applied field, resulting in a phase lag between the applied field and the polarization; energy is drawn from the electrical source, producing heat. Polarization losses add to conductive Ohmic losses and are represented using the imaginary relative permittivity, κ'' (Jonscher 1983; Hasted 1973; Hill et al. 1969; von Hippel 1954).

In summary, the relative permittivity is a measure of the extent to which the electrical charge distribution in the material can be distorted or polarized by the application of an electrical field. It is a complex parameter; the real part reflects the polarizability of the material, whereas the imaginary part characterizes Ohmic and polarization losses. Following the previous analysis, the complex polarization vector can be written as

$$\mathbf{P} = \epsilon_0(\kappa^* - 1)\mathbf{E} \tag{4}$$

where $\kappa^* = \kappa' - j\kappa''$ is the complex permittivity. The variation of the complex permittivity with frequency is called the "spectral response of the material" and depends on the nature of the polarization mechanism. There are several types of polarization mechanisms; the typical ones are: electronic, ionic, molecular, Maxwell-Wagner, and macrospace polarization (Fig. 1). In granular materials, backscatter at grain boundaries adds additional loss; this occurs when the wavelength approaches the particle diameter in the GHz region (Schaber et al. 1986). Polarizations that occur below this frequency are discussed next.

Applying an electric field to polar molecules, such as water, forces the randomly oriented molecules to align with the field, increasing the total polarization of the material at low frequencies. Debye (1929) described this type of polarization

$$\kappa^* = \kappa'_\infty + \frac{\kappa'_s - \kappa'_\infty}{1 + j\omega\tau} \tag{5}$$

where κ'_∞ is the optical permittivity, κ'_s is the static permittivity, ω is the angular frequency, and τ is the relaxation time.

Heterogeneous mixtures lead to relaxation behavior, even though the participating materials may not present spectral variations. This mechanism of polarization results from the difference in polarizability and conductivity of components, producing charge accumulation at interfaces. The result is a spatially polarized material. Using the Maxwell-Wagner electrical model, the following expression is obtained

$$\kappa^* = \kappa'_\infty + \frac{\kappa'_s - \kappa'_\infty}{1 + j\omega\tau} - j\frac{\sigma}{\omega\epsilon_0} \tag{6}$$

This equation differs from Debye's equation in the equivalent conductivity term, σ (von Hippel 1954).

Clay particles are electrically charged and form a double layer around them. Measurements of complex permittivity of colloidal suspensions show values as high as $\kappa' = 10^4$ at radio frequencies. This high value of permittivity was attributed to electrode polarization in early studies where films of molecular thickness form over the surface of electrodes, increasing the measured capacitance (Smith-Rose 1933). Verification of measurements with improved testing stimulated the development of new theories. O'Konski (1960), Schwarz (1962), Schurr (1964), and Lyklema et al. (1983) developed different models to explain high permittivity values for colloidal suspensions. Current theories propose that the applied external field displaces the center of the atmospheric charge from the center of the colloid, polarizing the double layer with respect to the clay particle.

Measurement of dielectric permittivity at different frequencies reveals different information. Permittivity at high frequencies (GHz) tests the free water in the system, whereas permittivity at low frequencies (high kHz and low MHz) detects changes in double layer polarization.

Mechanical Waves: Velocity of Propagation

Propagating mechanical waves examine the microstructure of the particulate medium at small strains. Velocity and attenuation

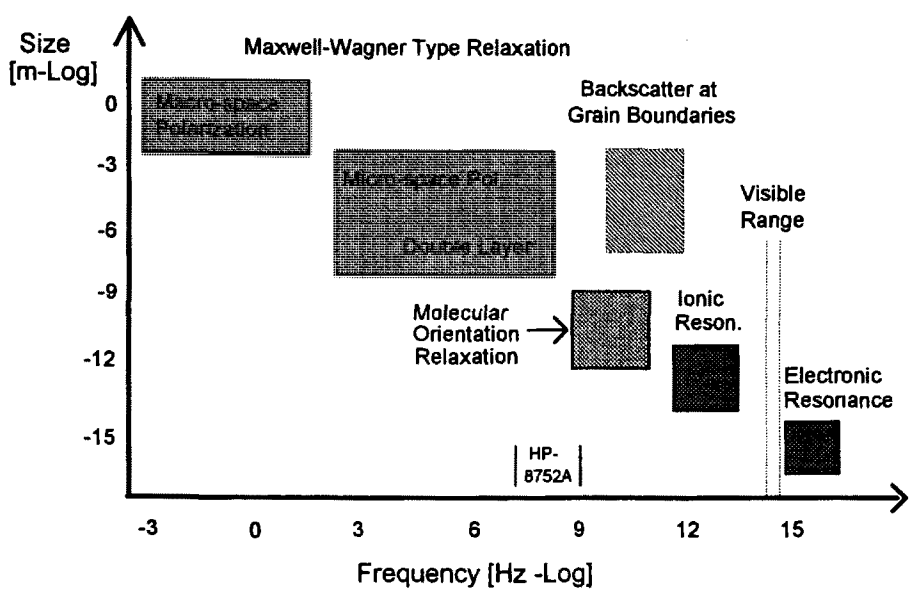

FIG. 1—*General trend between the size of the polarizing unit versus the characteristic frequency of the polarization. (Note region of backscatter at grain interphases.)*

reveal information about contacts, intergranular normal and shear forces, and the distribution of contact normals, which are determined by external stresses and internal processes.

In the case of saturated soils, shear waves propagate through the solid matrix with minimum influence from the pore fluid. This is not the case with compressional waves. Thus, shear waves are preferred to study the behavior of the soil matrix in saturated soils. On the other hand, attenuation is affected by pressure, porosity, degree of saturation, concentration, pore water viscosity, and material properties such as density and rigidity (Johnston 1981; Winkler and Nur 1981). Although attenuation may be more influenced than velocity during chemical and physical processes in geomaterials, measurement difficulties limit this paper to the monitoring of velocity changes.

Several experimental studies have been conducted to analyze the effect of the state of stress on the velocity of shear waves in particulate materials (Schultheiss 1981). As suggested by Roesler (1979) and Nishio and Tamaoki (1990), shear wave velocity is controlled by effective stresses in the direction of propagation and in the direction of polarization. A power equation was suggested by Roesler (1979) to relate shear wave velocity to stresses in the longitudinal and transverse directions, σ_l and σ_t, respectively,

$$V_s = \xi \cdot \left(\frac{\sigma_l}{p_a}\right)^{\chi l} \cdot \left(\frac{\sigma_t}{p_a}\right)^{\chi t} \tag{7}$$

where ξ, χ_l, and χ_t are constants, and p_a is the atmospheric pressure. In the case of an isotropic stress condition σ_{iso}, the previous equation reduces to

$$V_s = \xi \cdot \left(\frac{\sigma_{iso}}{p_a}\right)^{\gamma} \tag{8}$$

where the coefficient γ is equal to $\gamma = \chi_l + \chi_t$ (the coefficient γ is the slope of the log-log plot of velocity versus effective stress). Theoretical values for γ are predicted from contact theory: $\gamma = 1/6$ for spherical Hertzian contacts, and $\gamma = 1/4$ for cone-to-plane contacts (Gladwell 1980). Measurements of γ in real particulate materials show a variation from 0.16 to 0.48 (Aloufi and Santamarina 1995; Thomann and Hryciw 1990; Bates 1989; Schultheiss 1981).

Strains during the propagation of elastic mechanical waves are less than 10^{-5}, hence the micro structure of the material is not altered. Therefore, low-strain propagation reflects the stiffness of the given structure, which is determined by the type and distribution of contacts and by the state of stress. However, the large-strain modulus obtained from stress-strain tests characterizes the difficulty involved in producing microstructural changes in the system. In summary, the large-strain modulus characterizes "changes," however the low-strain modulus characterizes "state."

The coefficient γ is obtained from two or more measurements at different states of stress: *A, B,* ... etc. Even though waves do not alter the microstate, the change in stress from *A* to *B* does. Hence γ not only characterizes changes in contact stiffness but also changes in microfabric. Indeed, loose packings show higher γ than dense packings (Hryciw and Thomann 1993). In general, materials that have low large-strain moduli (i.e., soft clays) have a higher γ coefficient compared to stiffer materials such as quartz sands.

Oedometric Cell for Wave Measurements—Analysis

A special oedometer cell was designed and built. It incorporates transducers to measure shear wave velocity, dielectric permittivity, pore pressure, and temperature. Design criteria and analyses are discussed next.

Cell Design

The stainless steel shell, the Plexiglas base, and the brass upper plate were all machined with 0.05 mm tolerance. A porous stone was connected to the upper perforated plate to provide drainage. The base of the cell had three orifices to house the instrumentation. Configuration and dimensions of the cell are shown in Fig. 2.

Cell diameter and height were selected as a compromise between accuracy in travel time measurements, side friction, duration of time-dependent processes, and load capacity. The first model of the oedometer utilized a Plexiglas shell. Upon loading, cell expansion caused stress relaxation that affects velocity measurements. The improved device has a Grade 303 stainless steel shell.

Instrumentation—Calibration

The cell was mounted within a standard oedometer loading frame (Wykeham Farrance). Weights were used to apply the load through a calibrated lever arm. The vertical deformation of the specimen was monitored with a dial gage (0.002 mm). Other measurements were based on electronic circuitry.

Dielectric Permittivity—Capacitor-type probes allow for measurements in radio frequencies (double layer polarization); however, their design for continuous monitoring of processes is nontrivial. Alternatively, a coaxial termination probe was selected. It measured intensity and phase of reflected signals to determine the complex permittivity of the material. The probe (HP 85070A) was integrated with a network analyzer (HP 8752A). A PC computer was connected to the analyzer for control, acquisition, and storage. The probe works in the frequency range between 0.20 to 1.30 GHz (some measurements were extended to 0.02 GHz in the case of soils with high permittivity—personal communication with HP designers). This window captures the start of free water relaxation and the tail of double layer polarization (see Fig. 1). The depth of the tested material that affects permittivity measurements is inversely proportional to frequency and losses. In the case of this probe, the skin depth can be estimated as $20/\sqrt{\kappa'}$ mm. This small penetration gives "local" permittivity values.

The probe was calibrated every time before use. Calibration involved measuring open, short, and a known material (deionized water). The calibration process had to be performed with the probe at its final position since calibration is affected by the cable movements. The calibration was saved, and after the test was completed, it was verified to assess changes due to long-term drift.

Shear Wave Velocity—Piezocrystal bender elements (PZT-5, APC) were mounted on top and bottom platens to send and to receive shear waves. Crystals were insulated with a double coating of polyurethane (other coatings were tested but they showed short life in a moist environment). Bender elements were encapsulated inside a marine RTV resin to fix them to the base. A GR-1340 pulse generator was used to produce a square pulse in the lower bender element. The input pulse was also used to trigger a 20-MHz GOULD Digital Storage Oscilloscope 4035. Weak signals at high confining stresses were amplified with a 3944 KROHN-HITE Multi Channel Filter-Amplifier. A characteristic transmitted/received signal set is shown in Fig. 3. The travel time was measured twice for each pulse: at the start and at the end of the pulse.

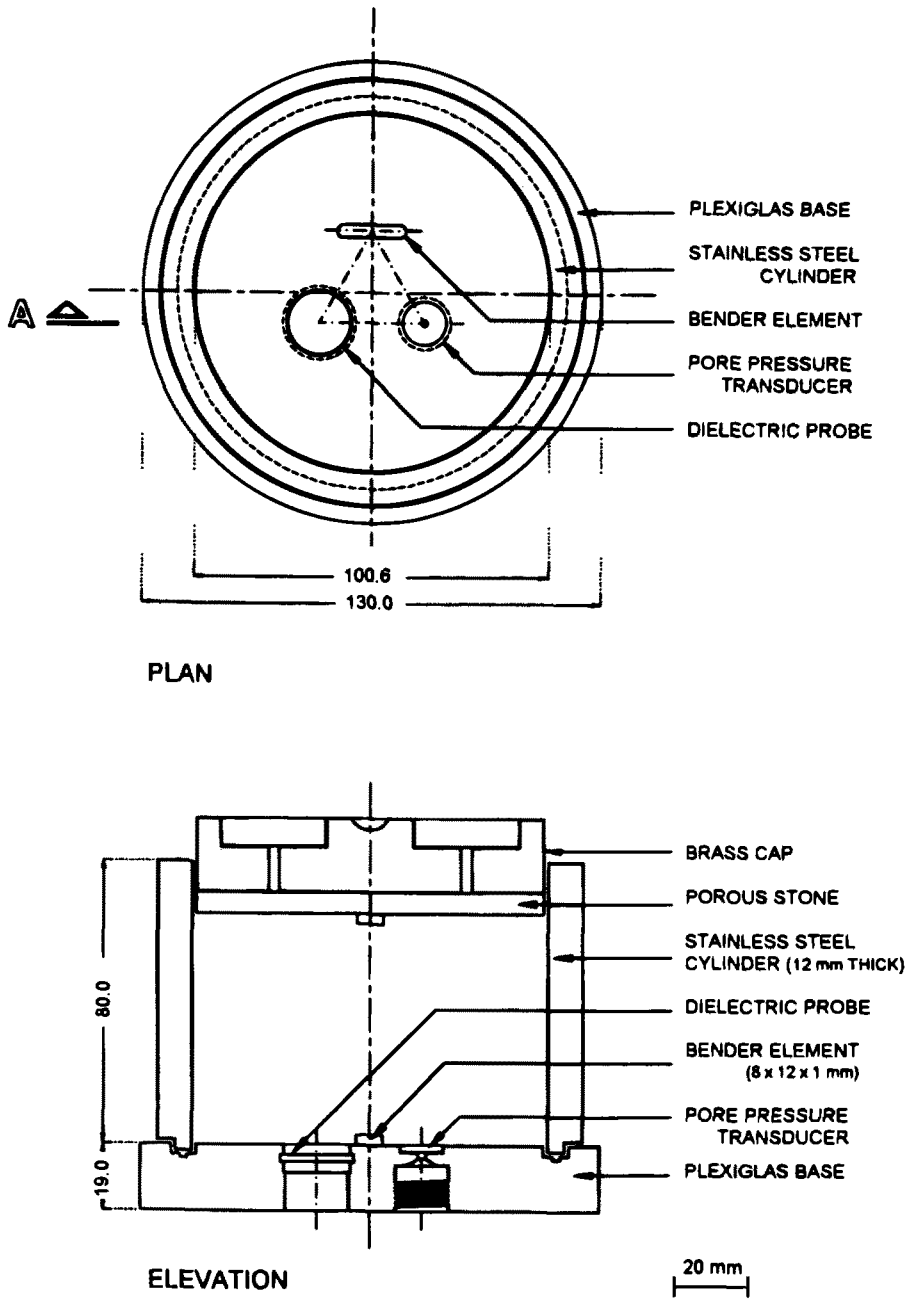

FIG. 2—*Oedometric cell: plan view and section elevation.*

Reversed polarity of received signals confirmed shear wave propagation (Kita et al. 1992).

Propagation is dispersive in repetitive media such as particulate or discrete geomaterials. If the wavelength approaches twice the spacing between particles, no energy is transmitted through the medium (Brillouin 1946). However, if the wavelength λ is much greater than the particle diameter, d, waves propagate through the medium as in a continuum. In this study, the frequency ranged between 10 to 30 kHz, varying with soil type and confining pressure. The corresponding wavelengths were $\lambda/d >> 1$.

Attenuation and amplitude scale on the screen affect the determination of the first arrival, and the error in travel time may exceed 5% (a commercial system to automatically measure travel time was tested, however, and displayed travel times could vary more than 20% depending on the selected threshold). All our measurements were conducted at maximum amplitude in the oscilloscope to assure consistency in picking first arrivals. The travel distance used in computing velocities was the distance between mid-heights of the free ends of the bender elements.

Pore Pressure—The pore pressure transducer, Dynisco PT25-2C, had an allowable pressure range between 0 to 1380 kPa. It was connected to a d-c power supply, and the output was read with a digital multimeter. The transducer was mounted at the base and detected only pore water pressure through a small diameter orifice (ID = 1.90 mm) that was covered by a rigid steel porous plate supported on the base. This design eliminates transmission of skeletal stresses.

Temperature—When processes under study were sensitive to temperature, a K-type thermocouple was installed inside the oedo-

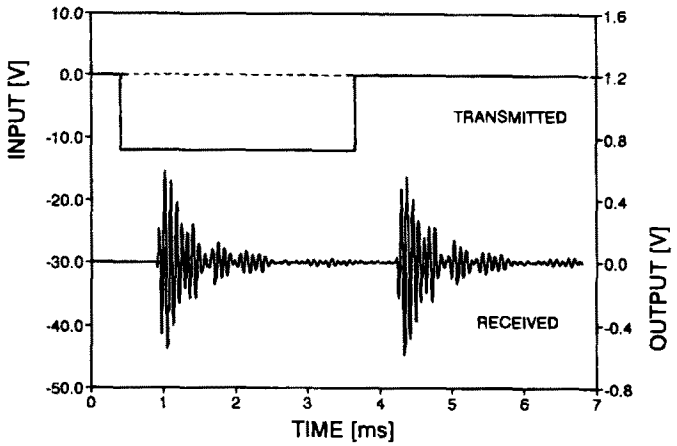

FIG. 3—*Determination of shear wave travel time: typical input function and received signal in kaolinite.*

meter. The tip of the thermocouple was coated with a thin layer of polyurethane. The temperature resolution was 0.1°C.

Local and Global Measurements—Analyses

Measurements can be classified under two categories: local, and global or depth averaging. Permittivity, pore water pressure, and temperature are local parameters. Shear wave velocity, deformation, and volume computations of water content and void ratio are global-average parameters. Correlations between parameters require local values.

Local values can be inverted from global measurements by combining boundary measurements and classical physical relations that govern the process under study, such as Terzaghi's consolidation theory or Fick's law of diffusion. For example, the average void ratio computed from the global volume can be inverted to local values using pore pressure measurements and Terzaghi's assumption of a linear relation between void ratio and excess pore water pressure (Terzaghi 1943)

$$e_l = e_f + (e_0 - e_f)\left(\frac{u_l}{u_0}\right) \tag{9}$$

where e_l is the local void ratio, e_0 is the initial void ratio before loading, e_f is the final void ratio at the end of consolidation, u_l is the local pore water pressure measured with the pore pressure transducer at the base of the specimen, and u_0 is the initial pore water pressure immediately after loading. Similar analyses can be applied to obtain local shear wave velocities from the average global-measured velocity or local permittivities across the specimen from local values measured at its base.

Processes Studied in the Modified Oedometer

The following sections present selected results on the monitoring of geotechnical processes with complementary mechanical and electromagnetic waves. The processes include consolidation, concentration diffusion, and cementation. (Physical and engineering properties of the tested soils are described in Santamarina and Fam 1995.)

Consolidation

A specimen of kaolinite was prepared using the slurry technique as described by Sheeran and Krizek (1971) and placed inside the modified oedometer. Changes in dielectric permittivity and shear wave velocity were recorded with time during consolidation under different stresses.

Dielectric Permittivity—A typical spectral plot for the complex permittivity of kaolinite during consolidation is shown in Fig. 4. The imaginary component at high frequency ($f > 0.6$ GHz) reflects the beginning of the free water relaxation, whereas losses at low frequency ($f < 0.4$ GHz) denounce the tail of the double layer polarization (refer to Fig. 1).

Figure 5 shows the evolution of the complex permittivity during a consolidation stage, from 305 to 610 kPa vertical effective stress. The change in real permittivity follows the change in the local water content (or void ratio) with time. The difference in real permittivity between low and high frequencies is approximately constant throughout the consolidation process. Considering that permittivity is the integration of all polarization mechanisms from high to low frequencies, it can be concluded that the consolidation of kaolinite at these stress levels affects only free water. The change in the imaginary permittivity confirms the reduction in free water since the high-frequency imaginary permittivity decreases with time, while the low-frequency imaginary permittivity remains approximately constant, showing no change in double layer polarization (Fam and Santamarina 1995).

Shear Wave Velocity—The global shear wave velocity was determined for each stress increment and plotted versus time. Figure 6 shows the change in shear velocity and void ratio for kaolinite during consolidation from 305 to 610 kPa vertical effective stress. Shear wave velocity reflects not only the increase in effective stress during primary consolidation, but may also reflect the increase in low strain stiffness during secondary consolidation.

Chemical Diffusion

The study and monitoring of chemical diffusion with wave techniques triggers important alternatives for lab and field testing. A kaolinite specimen was loaded to a vertical effective stress of 610 kPa, and then a saturated solution of potassium chloride was added and maintained at the top platen. The solution was allowed to diffuse one way into the soil. Permittivity and shear wave velocity were recorded with time.

Dielectric Permittivity—Complex permittivity during chemical diffusion is shown in Fig. 7. No change in the complex permittivity

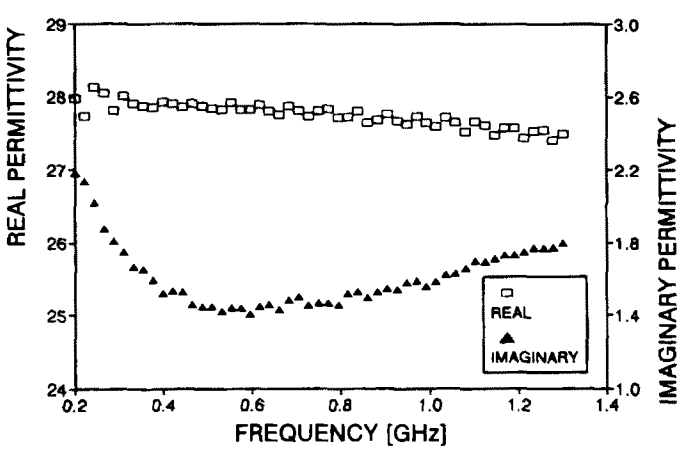

FIG. 4—*Consolidation: spectral permittivity for kaolinite at 610 kPa vertical effective stress.*

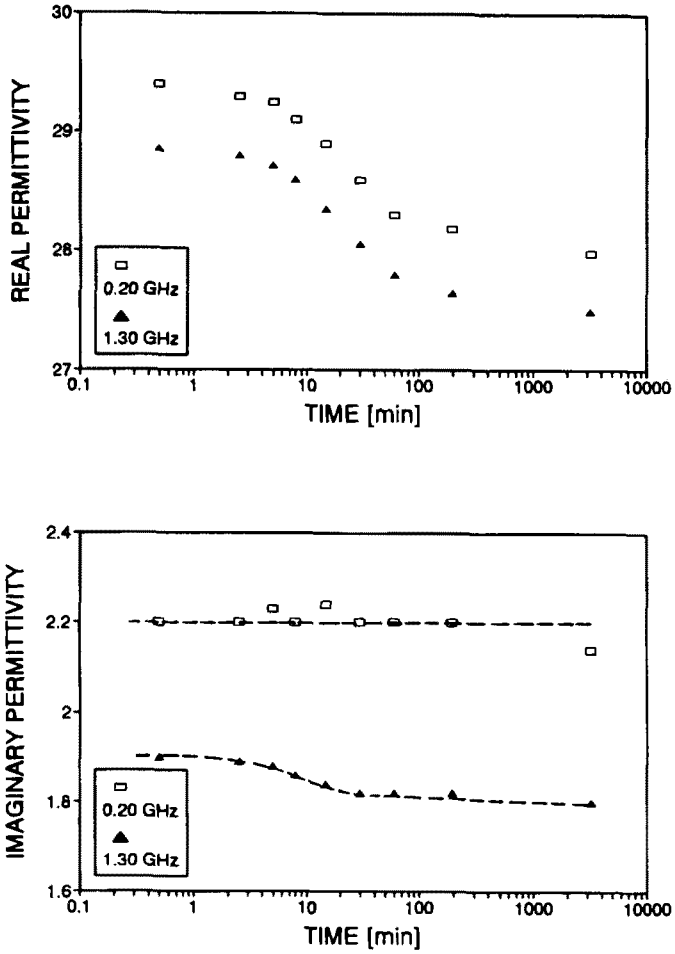

FIG. 5—*Consolidation and complex permittivity: change in the real and imaginary permittivity of kaolinite from 305 to 610 kPa vertical effective stress versus time at two different frequencies.*

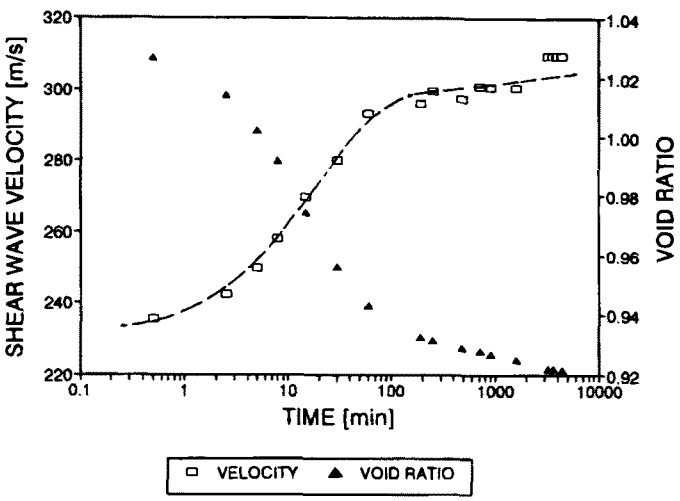

FIG. 6—*Consolidation and shear wave velocity: evolution of average velocity and void ratio during consolidation of kaolinite from 305 to 610 kPa vertical effective stress.*

of kaolinite was observed until the chemical front approached the skin depth of the probe. At this time, the real permittivity at 1.30 GHz decreased slightly, responding to the decrease in free water (Barbour and Fredlund 1989). The increase in real permittivity at 0.2 GHz may be the biasing of κ' by high κ'' at low frequency.

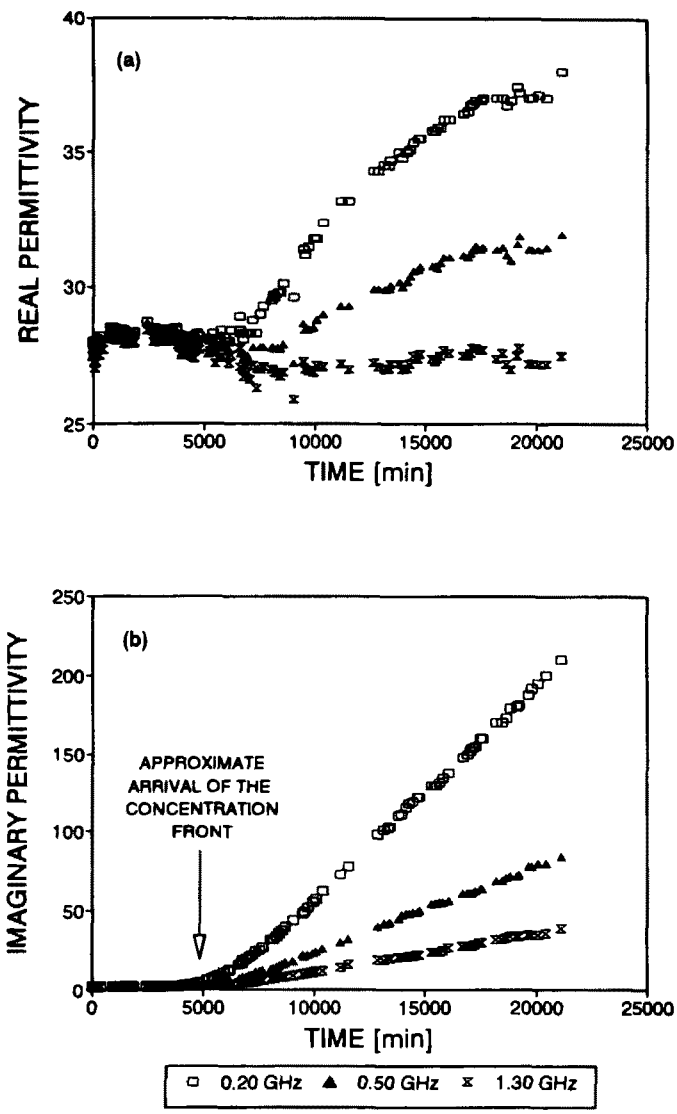

FIG. 7—*Chemical diffusion and complex permittivity: kaolinite at 610 kPa vertical effective stress subjected to one-way diffusion of a saturated solution of potassium chloride:* (a) *real;* (b) *imaginary.*

On the contrary, the imaginary permittivity changed significantly (Fig. 7*b*). The increase in the imaginary permittivity results primarily from the increase in d-c losses as the concentration increases; this overcompensates for the reduction in double layer polarization.

Shear Wave Velocity—The change in shear wave velocity in kaolinite during chemical diffusion is shown in Fig. 8. Shear wave velocity decreased by 10%. Different possible mechanisms may combine and affect shear wave propagation. The shrinkage of clay with the increase in concentration may produce lateral stress relaxation, reducing shear wave velocity according to Eq 7. Other possible mechanisms are related to changes in true effective stresses and short-range forces as a result of the increase in concentration. The relative effects of these factors are described in Santamarina and Fam (1995).

Cementation: Clay-Cement Mixtures

Surface permittivity measurements of clay-cement mixtures are very sensitive to probe penetration inside the specimen. Therefore,

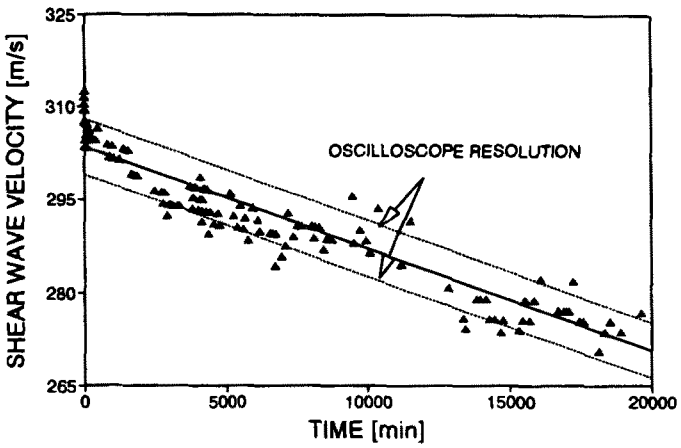

FIG. 8—*Chemical diffusion and shear wave velocity: kaolinite at 610 kPa vertical effective stress subjected to one-way diffusion of a saturated solution of potassium chloride.*

the modified oedometer presents a unique tool to obtain well-controlled permittivity and shear wave velocity measurements. A bentonite-cement mixture was prepared by prehydrating bentonite at 1200% water:bentonite ratio and mixing it with cement to a 1:1 bentonite:cement ratio (by weight). The slurry was poured into the modified oedometer. A vertical pressure equal to 2.50 kPa was applied. Temperature changes during hydration were monitored.

Dielectric Permittivity—Figure 9 shows complex permittivity results at high frequency (1.30 GHz). A continuous decrease in real permittivity is observed. This is in agreement with measurements of cement mortar at 10 GHz by Moukwa et al. (1991). The overall decrease in dielectric permittivity with time at this frequency can be explained with different hypotheses including: reduction in free water due to consolidation, the change of free water into bound water due to cement hydration, a decrease in permittivity as a result of the increase in concentration and, finally, thermal effects on permittivity.

The change in the imaginary permittivity at 1.30 GHz is shown in Fig. 9. Three different stages can be observed. During the first stage (30 min), a "leaky" impermeable membrane of bentonite particles forms around cement particles, thus, κ'' increases at low rate as conductivity increases. The second stage (300 to 700 min) is characterized by the active reaction between cement and water after the collapse of the clay shell around cement particles or due to the breakdown of the clay particle by lime liberation (Mitchell and El Jack 1965). During this stage, the real permittivity decreases due to loss of free water in the hydrating clay and cement; the imaginary permittivity increases because of higher d-c and double layer losses. Finally, the third stage (after 700 min) shows a gradual decrease in both real and imaginary permittivity because of the decrease in free water due to crystallization and the formation of hydrated calcium-silicates.

Shear Wave Velocity—The evolution of shear wave velocity in the bentonite-cement mixture is shown in Fig. 10. The increase in shear wave velocity with time reflects the increase in cementation between particles, higher contact rigidity, and consolidation process (the shear wave velocity of a water-bentonite mixture without the cement at this state of stress is approximately 20 m/s and consolidation requires approximately four days to complete). Shear modulus curves obtained for cement mortar by Matsufuji and Kawakami (1984) are significantly different from velocity-time curves measured in this study, highlighting the different roles of

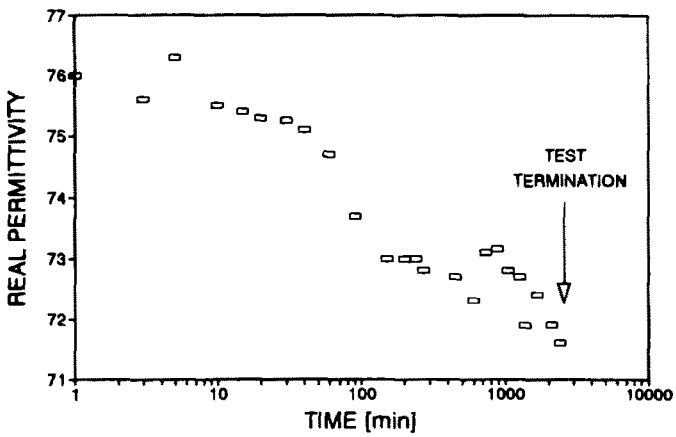

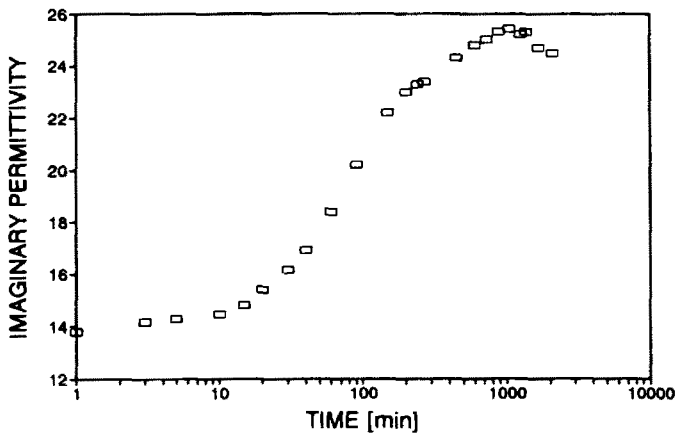

FIG. 9—*Cementation and complex permittivity: evolution of the real and imaginary permittivity of bentonite-cement mixture 1:1 by weight, at water/clay = 1200%, vertically loaded with 2.5 kPa.*

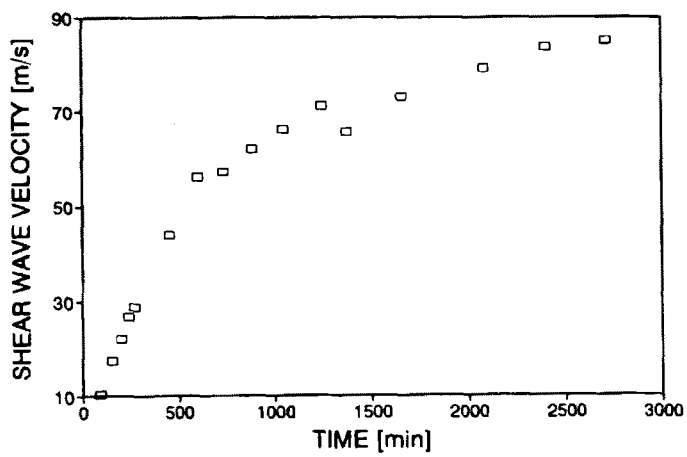

FIG. 10—*Cementation and shear wave velocity: evolution of the wave velocity in bentonite-cement mixture 1:1 by weight, at water/clay = 1200%, vertically loaded with 2.5 kPa.*

inert aggregates as compared to surface-charged, high-specific-surface bentonites. Note that shear wave velocity gives little insight about changes in the nature of water and the chemical processes occurring in the mixture.

Final Comments and Recommendations

Measurements with mechanical and electromagnetic waves add significant insight into the materials under study. Wave techniques can not only be used to monitor different processes, but also to investigate phenomena behind processes. Proper interpretation of the information revealed using wave techniques requires clear understanding of wave-material interaction and comprehension of wave propagation concepts.

There are important applications for such dual measurements in geotechnical, geoenvironmental, mining, and agricultural engineering. Distinctive processes that can be studied or monitored with this methodology include: the interaction between clay liners and chemically active waste; creep densification of granular salt fill during the gradual closure of caverns in salt beds; physical and chemical changes in coal mines and mine tailings; consolidation of oil-saturated porous media in compaction-driven oil production; electroosmosis and the effects of changes in true effective stress, moisture, and temperature; loading, aging, wet-dry cycles, and rotting of food grains. In all these cases, wave-based measurements may be combined with inversion mathematics to develop advanced laboratory or field applications.

Acknowledgments

This study is part of a research program on wave-geomedia interaction and applications. Funding is provided by the Natural Sciences and Engineering Research Council of Canada, NSERC. Assistance by Hewlett-Packard is gratefully acknowledged.

References

Aloufi, M. and Santamarina, J. C., 1995, "Low and High Strain Macrobehavior of Grain Masses—The Effect of Particle Eccentricity," *American Society of Agricultural Engineering ASAE,* Vol. 38, No. 3, p. 877.

Barbour, S. L. and Fredlund, D. G., 1989, "Mechanisms of Osmotic Flow and Volume Change in Clay Soils," *Canadian Geotechnical Journal,* Vol. 26, pp. 551–562.

Bates, C. R., 1989, "Dynamic Soil Property Measurements During Triaxial Testing," *Geotechnique,* Vol. 39, No. 4, pp. 721–726.

Brillouin, L., 1946, *Wave Propagation in Periodic Structures,* McGraw Hill, New York.

Debye, P., 1929, *Polar Molecules,* Chemical Catalog Company, New York.

Fam, M., 1995, "Study of Physico-Chemical Processes with Mechanical and Electromagnetic Waves," thesis submitted for the partial fulfillment of Ph.D. degree, University of Waterloo.

Fam, M. and Santamarina, J. C., 1995, "A Study of Consolidation Using Mechanical and Electromagnetic Waves," *Geotechnique,* under review.

Gladwell, G. M. L., 1980, *Contact Problems in the Classical Theory of Elasticity,* Sijthoff and Noordhoff, Germantown, Maryland.

Hasted, J. B., 1973, *Aqueous Dielectrics,* Chapman and Hall, London.

Hill, N. E., Vaughan, W. E., and Davis, M., 1969, *Dielectric Properties and Molecular Behavior,* Van Nostrand Reinhold Company, London.

Hryciw, R. D. and Thomann, T. G., 1993, "A Stress-History-Based Model for the G^e of Cohesionless Soils," *Journal of Geotechnical Engineering, ASCE,* Vol. 119, No. 7, p. 1073.

Johnston, D. H., 1981, "Attenuation: A State-of-the Art Summary," Society of Exploration Geophysics, M. N. Toksoz and D. H. Johnston, Eds., *Geophysics Reprint Series,* No. 2, pp. 123–135.

Jonscher, A. K., 1983, *Dielectric Relaxation in Solids,* Chelsea Dielectric Press, London.

Kita, K., Shibata, T., Yashima, A., and Kobayashi, S., 1992, "Measurement of Shear Wave Velocities of Sand in a Centrifuge," *Soils and Foundations,* Vol. 32, No. 2, pp. 134–140.

Lyklema, J., Dukhin, S. S., and Shilov, V. N., 1983, "The Relaxation of the Double Layer Around Colloidal Particles and the Low-Frequency Dielectric Dispersion," *Journal of Electroanalytical Chemistry,* Vol. 143, pp. 1–20.

Matsufuji, Y. and Kawakami, 1984, "A Study on the Evaluating Method of Setting Condition of Concrete Mixtures by Shear Wave Propagation Characteristics," *Proceedings,* Twenty-Eighth Japan Congress on Material Research, Science Council of Japan, National Council of Materials Research, Kyoto.

Mitchell, J. K. and El Jack, S. A., 1965, "The Fabric of Soil-Cement and Its Formation," *Proceedings,* Fourteenth National Conference on Clays and Clay Minerals, Pergamon, Elmsford, NY, pp. 297–305.

Moukwa, M., Brodwin, M., Christo, S., Chang, J., and Shah, S. P., 1991, "The Influence of the Hydration Process Upon Microwave Properties of Cements," *Cement and Concrete Research,* Vol. 21, pp. 863–872.

Nishio, S. and Tamaoki, K., 1990, "Stress Dependency of Shear Wave Velocities in Diluvial Gravel Samples During Triaxial Compression Tests," *Soils and Foundations,* Vol. 30, No. 4, pp. 42–52.

O'Konski, C. T., 1960, "Electric Properties of Macromolecules. V. Theory of Ionic Polarization in Polyelectrolytes," *Journal of Physical Chemistry,* Vol. 64, pp. 605–618.

Roesler, S. K., 1979, "Anisotropic Shear Modulus Due to Stress Anisotropy," *Journal of Geotechnical Engineering, ASCE,* Vol. 105, No. GT7, pp. 871–880.

Santamarina, J. C. and Fam, M., 1995, "Changes in Dielectric Permittivity and Shear Wave Velocity During Concentration Diffusion," *Canadian Geotechnical Journal,* Vol. 32, No. 4.

Schaber, G. G., McCauley, J. F., Breed, C. S., and Olhoeft, G. R., 1986, "Shuttle Imaging Radar: Physical Controls on Signal Penetration and Subsurface Scattering in the Eastern Sahara," *IEEE Transactions on Geoscience and Remote Sensing,* Vol. GE-24, No. 4, pp. 603–623.

Schultheiss, P. J., 1981, "Simultaneous Measurements of P & S Wave Velocities During Conventional Laboratory Soil Testing Procedures," *Marine Geotechnology,* Vol. 4, No. 4, pp. 343–367.

Schurr, J. M., 1964, "On the Theory of the Dielectric Dispersion of Spherical Colloidal Particles in Electrolyte Solution," *Journal of Physical Chemistry,* Vol. 68, pp. 2407–2413.

Schwarz, G., 1962, "A Theory of the Low-frequency Dielectric Dispersion of Colloidal Particles in Electrolyte Solution," *Journal of Physical Chemistry,* Vol. 66, pp. 2636–2642.

Sheeran, D. E. and Krizek, R. J., 1971, "Preparation of Homogeneous Soil Samples by Slurry Consolidation," *Journal of Materials,* JMLSA, Vol. 6, No. 2, June, pp. 356–373.

Smith-Rose, R. L., 1933, "The Electrical; Properties of Soil for Alternating Currents at Radio Frequencies," *Proceedings Royal Society,* Vol. 140, pp. 359–377.

Terzaghi, K., 1943, *Theoretical Soil Mechanics,* John Wiley and Sons, New York.

Thomann, T. G. and Hryciw, R., 1990, "Laboratory Measurement of Small Strain Shear Modulus under Ko Condition," *Geotechnical Testing Journal,* Vol. 13, No. 2, June, pp. 97–105.

von Hippel, A. R., 1954, *Dielectric and Waves,* John Wiley & Sons, Inc., first student edition.

Winkler, K., Nur, A., and Gladwin, M., 1981, "Friction and Seismic Attenuation in Rocks," Society of Exploration Geophysics, M. N. Toksoz and D. H. Johnston, Eds., *Geophysics Reprint Series,* No. 2, pp. 115–118.